Temperature and radiative responses to anthropogenic aerosols over the Mediterranean Basin based on CMIP6 Earth system models

Alkiviadis Kalisoras[1], Prodromos Zanis[1], Aristeidis K. Georgoulias[1,2], Dimitris Akritidis[1], Robert J. Allen[3], Vaishali Naik[4]

[1]Department of Meteorology and Climatology, School of Geology, Aristotle University of Thessaloniki, Thessaloniki, Greece
[2]Climate and Atmosphere Research Center, The Cyprus Institute, Nicosia, Cyprus
[3]Department of Earth and Planetary Sciences, University of California Riverside, Riverside, CA, USA
[4]NOAA Geophysical Fluid Dynamics Laboratory, Princeton, NJ, USA

Correspondence to: Alkiviadis Kalisoras (kalisort@geo.auth.gr)

This is the electronic supplement of the article "Temperature and radiative responses to anthropogenic aerosols over the Mediterranean Basin based on CMIP6 Earth system models".

Table S1. Annual mean values (in W m^{-2}) of shortwave (SW), longwave (LW) and net (SW+LW) atmospheric radiative cooling (ARC) at the top-of-atmosphere (TOA) and for the entire atmospheric column over the Mediterranean for the periods 1970-1979, 2005-2014 and their difference (2005-2014 minus 1970-1979). Values are presented for each model, along with the multi-model ensemble mean and the inter-model variability (one standard deviation; SD).

Model	1970-1979						2005-2014						2005-2014 minus 1970-1979					
	TOA SW	TOA LW	TOA NET	SW	LW	NET	TOA SW	TOA LW	TOA NET	SW	LW	NET	TOA SW	TOA LW	TOA NET	SW	LW	NET
BCC-ESM1	7.98	-5.26	2.72	-0.03	-3.59	-3.62	5.55	-5.15	0.40	-0.32	-4.01	-4.34	-2.43	0.11	-2.32	-0.29	-0.43	-0.72
CNRM-ESM2-1	4.18	-2.07	2.12	-0.83	-0.52	-1.35	2.60	-1.39	1.21	-1.01	-0.06	-1.08	-1.59	0.68	-0.91	-0.18	0.46	0.28
EC-Earth3-AerChem	8.60	-8.00	0.60	-0.61	-5.17	-5.78	5.44	-6.21	-0.77	-2.34	-3.01	-5.35	-3.16	1.80	-1.36	-1.73	2.16	0.43
GFDL-ESM4	6.42	-3.40	3.02	-1.64	-0.62	-2.26	3.93	-2.54	1.39	-2.13	-0.72	-2.84	-2.49	0.87	-1.63	-0.48	-0.09	-0.58
MPI-ESM-1-2-HAM	7.77	-3.00	4.78	-0.39	-0.63	-1.02	5.40	-3.41	1.99	-1.17	-0.85	-2.02	-2.37	-0.41	-2.79	-0.78	-0.23	-1.01
MRI-ESM2-0	9.73	-3.56	6.17	-0.13	-1.83	-1.95	3.86	-1.93	1.93	-0.28	-2.43	-2.71	-5.87	1.63	-4.24	-0.15	-0.61	-0.76
NorESM2-LM	5.25	-4.07	1.19	-0.23	-2.00	-2.23	2.88	-2.31	0.57	-0.79	-1.30	-2.09	-2.37	1.76	-0.61	-0.56	0.70	0.14
UKESM1-0-LL	7.84	-6.47	1.37	-0.47	-3.26	-3.74	4.71	-5.07	-0.36	-1.76	-2.01	-3.77	-3.12	1.39	-1.73	-1.29	1.26	-0.04
Ensemble (Mean)	7.22	-4.48	2.75	-0.54	-2.20	-2.74	4.30	-3.50	0.80	-1.23	-1.80	-3.03	-2.93	0.98	-1.95	-0.68	0.40	-0.28
Ensemble (SD)	1.70	1.84	1.78	0.48	1.58	1.46	1.09	1.65	0.95	0.73	1.23	1.30	1.20	0.76	1.09	0.53	0.88	0.51

Table S2. As in Table S1, but for the boreal winter (DJF).

Model	1970-1979						2005-2014						2005-2014 minus 1970-1979					
	TOA SW	TOA LW	TOA NET	SW	LW	NET	TOA SW	TOA LW	TOA NET	SW	LW	NET	TOA SW	TOA LW	TOA NET	SW	LW	NET
BCC-ESM1	3.63	-2.34	1.29	0.15	-1.26	-1.11	3.51	-4.12	-0.61	0.00	-2.20	-2.20	-0.12	-1.78	-1.90	-0.15	-0.94	-1.09
CNRM-ESM2-1	2.49	-1.65	0.84	-0.34	-0.49	-0.84	1.38	-0.52	0.86	-0.39	-0.32	-0.71	-1.11	1.13	0.02	-0.04	0.17	0.13
EC-Earth3-AerChem	7.78	-5.87	1.90	-0.48	-3.00	-3.48	3.05	-1.28	1.77	-0.91	0.50	-0.40	-4.73	4.60	-0.13	-0.42	3.51	3.08
GFDL-ESM4	3.99	-2.79	1.20	-1.05	0.64	-0.41	1.21	-0.57	0.64	-1.31	0.93	-0.38	-2.78	2.22	-0.56	-0.27	0.30	0.03
MPI-ESM-1-2-HAM	7.62	-2.60	5.02	-0.55	1.44	0.89	2.61	1.23	3.84	-0.44	1.78	1.34	-5.01	3.83	-1.18	0.11	0.34	0.45
MRI-ESM2-0	6.91	-3.02	3.88	0.18	0.38	0.56	2.82	-2.17	0.65	-0.22	-0.78	-1.01	-4.09	0.86	-3.24	-0.41	-1.16	-1.57
NorESM2-LM	3.42	-2.55	0.88	-0.25	-0.30	-0.55	3.81	-2.79	1.02	-0.42	-1.01	-1.43	0.39	-0.24	0.15	-0.17	-0.71	-0.88
UKESM1-0-LL	4.88	-4.64	0.24	-0.24	-1.33	-1.57	4.32	-5.01	-0.69	-0.78	-1.11	-1.89	-0.56	-0.36	-0.93	-0.54	0.22	-0.32
Ensemble (Mean)	5.09	-3.18	1.91	-0.32	-0.49	-0.81	2.84	-1.90	0.94	-0.56	-0.27	-0.83	-2.25	1.28	-0.97	-0.24	0.21	-0.02
Ensemble (SD)	1.93	1.29	1.56	0.37	1.29	1.27	1.03	1.91	1.34	0.39	1.20	1.03	2.03	2.03	1.07	0.20	1.37	1.33

Table S3. As in Table S1, but for the boreal summer (JJA).

Model	1970-1979						2005-2014						2005-2014 minus 1970-1979					
	TOA SW	TOA LW	TOA NET	SW	LW	NET	TOA SW	TOA LW	TOA NET	SW	LW	NET	TOA SW	TOA LW	TOA NET	SW	LW	NET
BCC-ESM1	11.72	-9.21	2.51	-0.46	-6.56	-7.02	5.84	-6.28	-0.44	-0.58	-5.14	-5.72	-5.89	2.94	-2.95	-0.12	1.42	1.30
CNRM-ESM2-1	7.04	-3.84	3.20	-1.76	-0.97	-2.72	3.56	-2.01	1.55	-1.76	0.10	-1.66	-3.48	1.83	-1.65	-0.01	1.07	1.06
EC-Earth3-AerChem	9.85	-12.09	-2.24	-0.88	-9.43	-10.31	7.27	-11.75	-4.48	-4.30	-6.49	-10.80	-2.58	0.34	-2.23	-3.43	2.94	-0.49
GFDL-ESM4	8.98	-5.66	3.31	-2.68	-2.36	-5.04	5.19	-4.19	1.00	-2.80	-2.81	-5.61	-3.79	1.47	-2.32	-0.12	-0.44	-0.57
MPI-ESM-1-2-HAM	8.24	-6.12	2.12	-0.50	-3.83	-4.33	4.79	-5.30	-0.51	-1.80	-2.80	-4.59	-3.45	0.82	-2.63	-1.29	1.03	-0.26
MRI-ESM2-0	11.75	-5.36	6.39	-0.62	-4.84	-5.46	5.12	-2.85	2.27	-0.21	-4.33	-4.55	-6.63	2.51	-4.12	0.40	0.51	0.91
NorESM2-LM	5.67	-5.33	0.34	-0.48	-2.88	-3.36	2.41	-2.46	-0.05	-1.23	-1.53	-2.76	-3.26	2.87	-0.39	-0.75	1.35	0.60
UKESM1-0-LL	9.21	-9.07	0.13	-0.88	-5.90	-6.78	4.19	-5.66	-1.47	-2.63	-2.88	-5.51	-5.02	3.41	-1.60	-1.75	3.02	1.27
Ensemble (Mean)	9.06	-7.09	1.97	-1.03	-4.60	-5.63	4.80	-5.06	-0.27	-1.91	-3.23	-5.15	-4.26	2.03	-2.24	-0.88	1.36	0.48
Ensemble (SD)	1.98	2.58	2.42	0.74	2.52	2.26	1.37	2.92	1.96	1.23	1.94	2.53	1.33	1.02	1.02	1.17	1.08	0.74

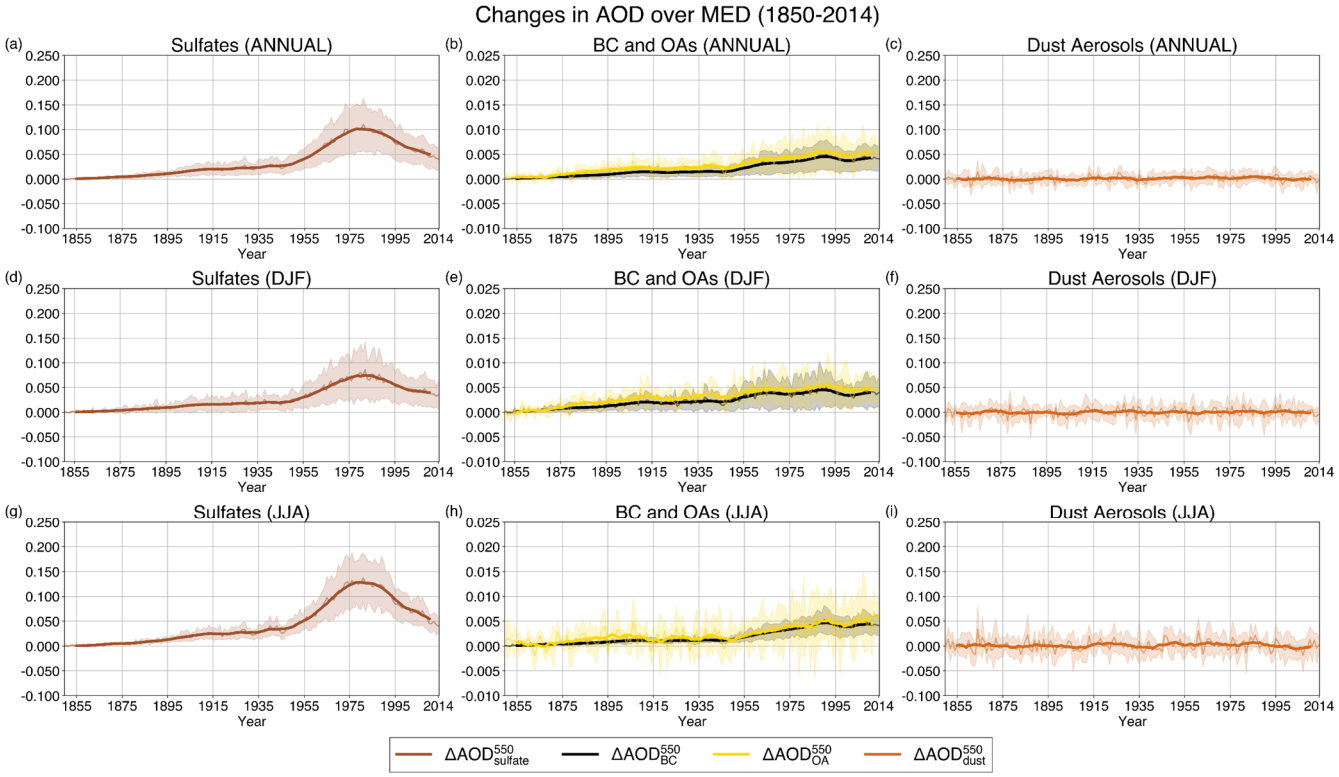

Figure S1. Timeseries of the AA-induced evolution of the aerosol optical depth (AOD) of sulfate aerosols (left column) black carbon (BC) and organic aerosols (OA; middle column), and dust aerosols (right column) over the Mediterranean region (10°W-40°E, 30°N-45°N) for the historical period (1850-2014) on an annual scale (top row) and in boreal winter (DJF; middle row) and summer (JJA; bottom row). Changes in AOD were calculated from the difference "historical" minus "hist-piAer". The thin lines represent the annual weighted mean values, while thick lines represent the 10-year moving average. Shading expresses the inter-model variability (one standard deviation).

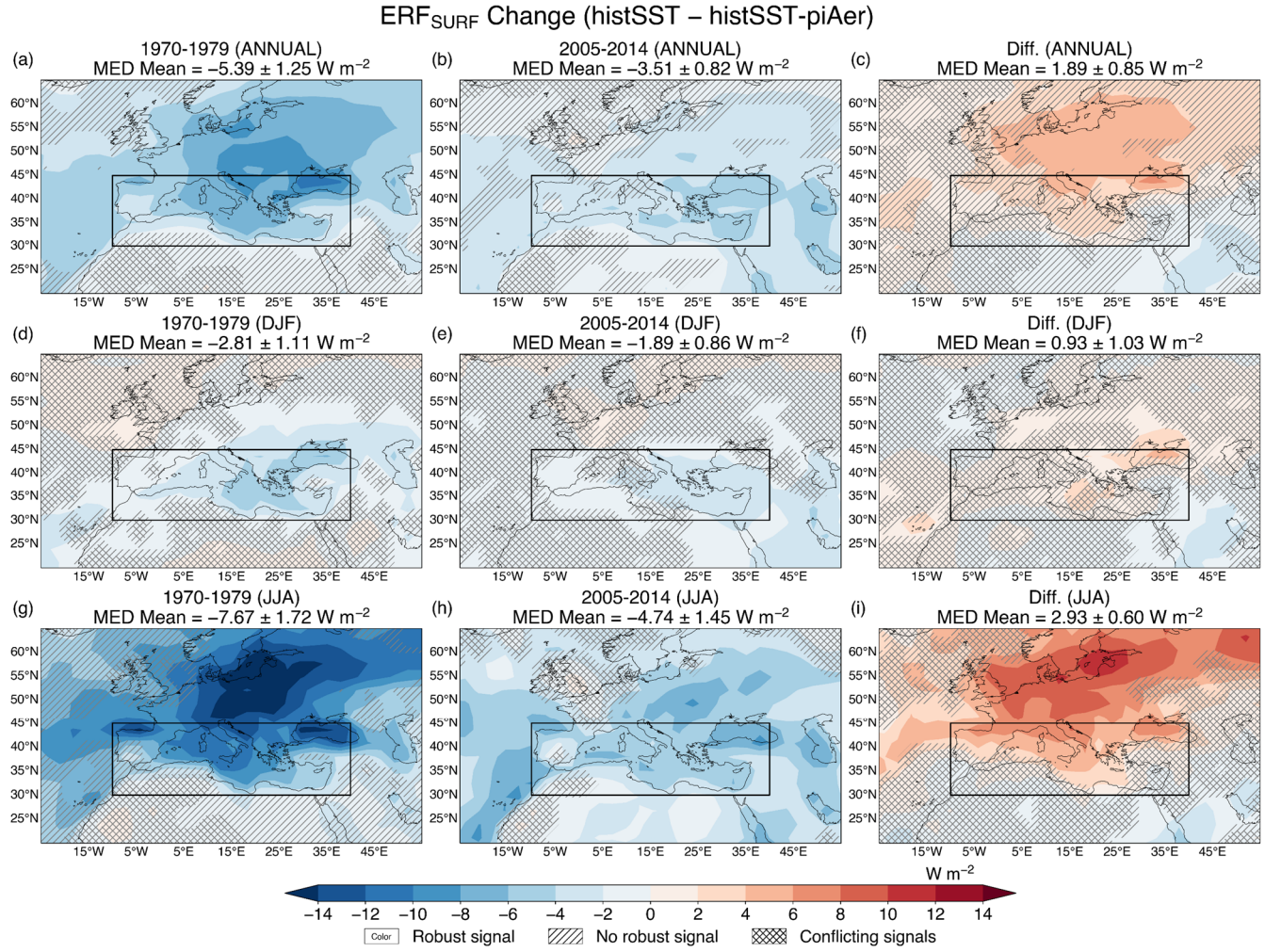

Figure S2. ERF$_{SURF}$ due to anthropogenic aerosols (calculated from the difference "histSST" minus "histSST-piAer") over the Mediterranean (in W m^{-2}). Spatial patterns are presented for the periods 1970-1979 (left column), 2005-2014 (middle column) and their difference (2005-2014 minus 1970-1979; right column) on an annual scale (top row) and in boreal winter (DJF; middle row) and summer (JJA; bottom row). The multi-model ensemble means over the Mediterranean region (shown as a box) are shown along with the inter-model variability (one standard deviation) at the top of each panel. Colored areas without markings indicate robust changes, while hatched (/) and cross-hatched (X) areas indicate non-robust changes and conflicting signals, respectively.

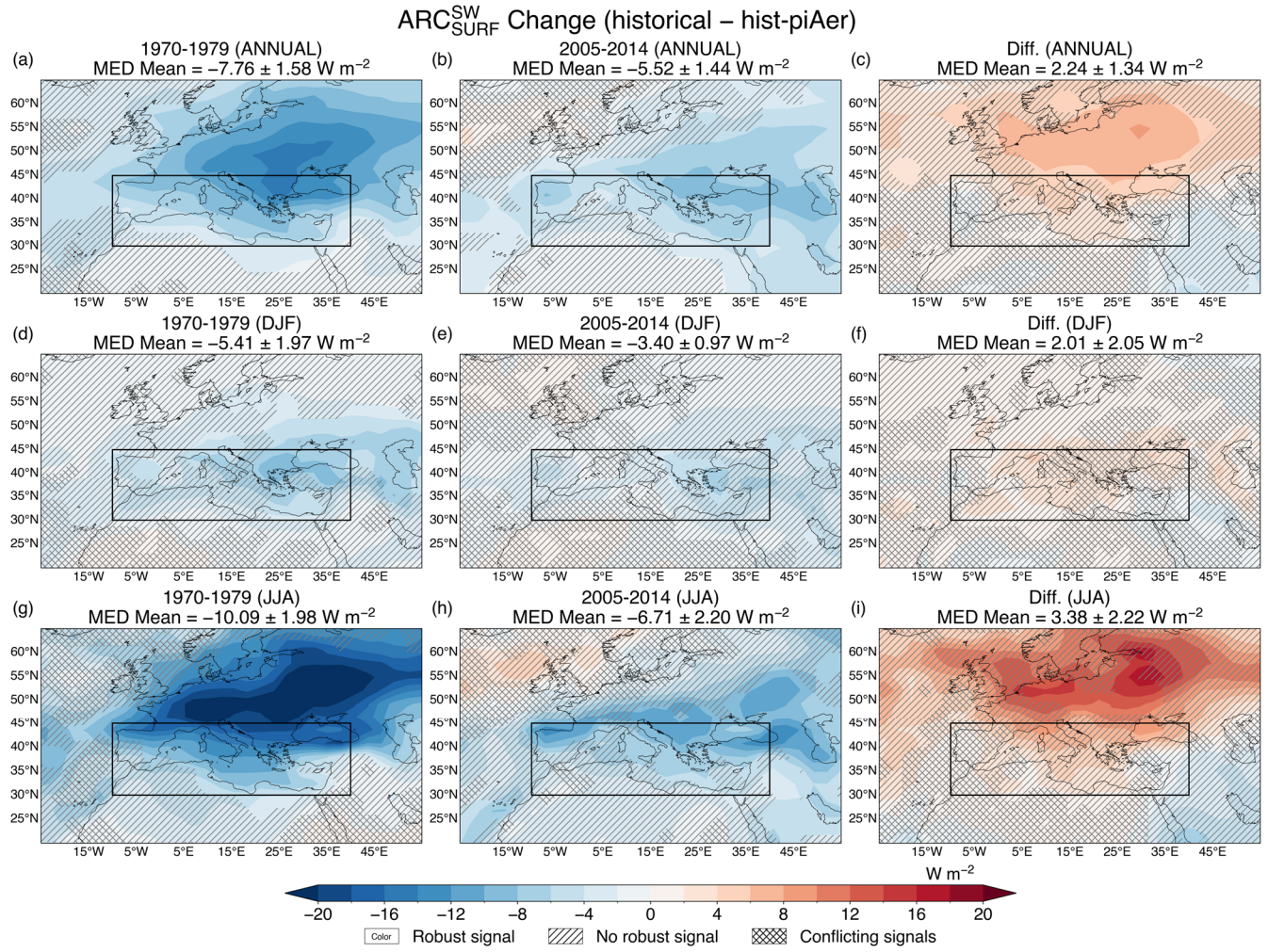

Figure S3. Shortwave (SW) ARC_{SURF} due to anthropogenic aerosols over the Mediterranean (calculated from the difference "historical" minus "hist-piAer"). Spatial patterns are presented for the periods 1970-1979 (left column), 2005-2014 (middle column) and their difference (2005-2014 minus 1970-1979; right column) on an annual scale (top row) and in boreal winter (DJF; middle row) and summer (JJA; bottom row). The multi-model ensemble means over the Mediterranean region (shown as a box) are shown along with the inter-model variability (one standard deviation) at the top of each panel. Colored areas without markings indicate robust changes, while hatched (/) and cross-hatched (X) areas indicate non-robust changes and conflicting signals, respectively.

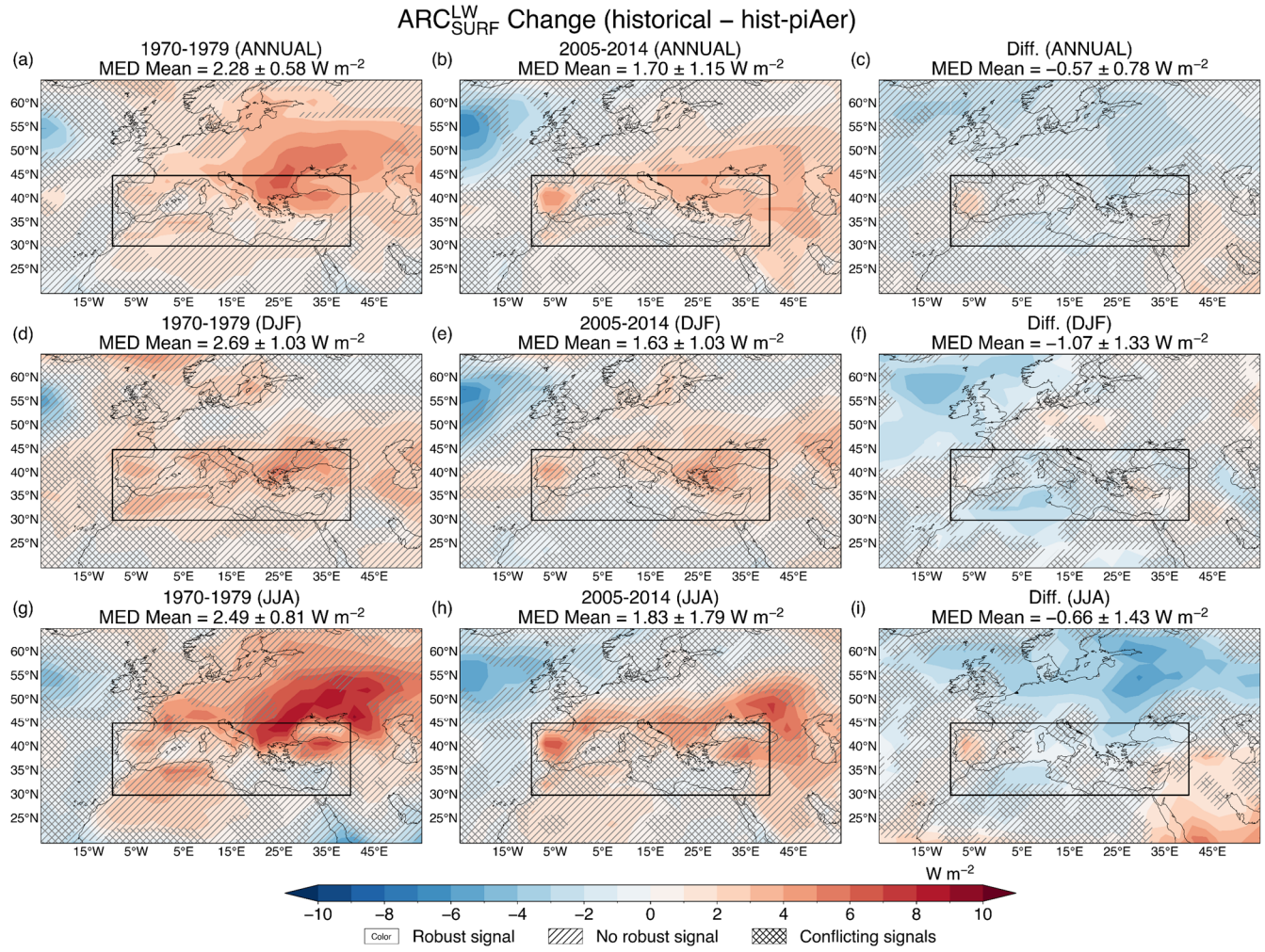

Figure S4. Longwave (LW) ARC_{SURF} due to anthropogenic aerosols over the Mediterranean (calculated from the difference "historical" minus "hist-piAer"). Spatial patterns are presented for the periods 1970-1979 (left column), 2005-2014 (middle column) and their difference (2005-2014 minus 1970-1979; right column) on an annual scale (top row) and in boreal winter (DJF; middle row) and summer (JJA; bottom row). The multi-model ensemble means over the Mediterranean region (shown as a box) are shown along with the inter-model variability (one standard deviation) at the top of each panel. Colored areas without markings indicate robust changes, while hatched (/) and cross-hatched (X) areas indicate non-robust changes and conflicting signals, respectively.

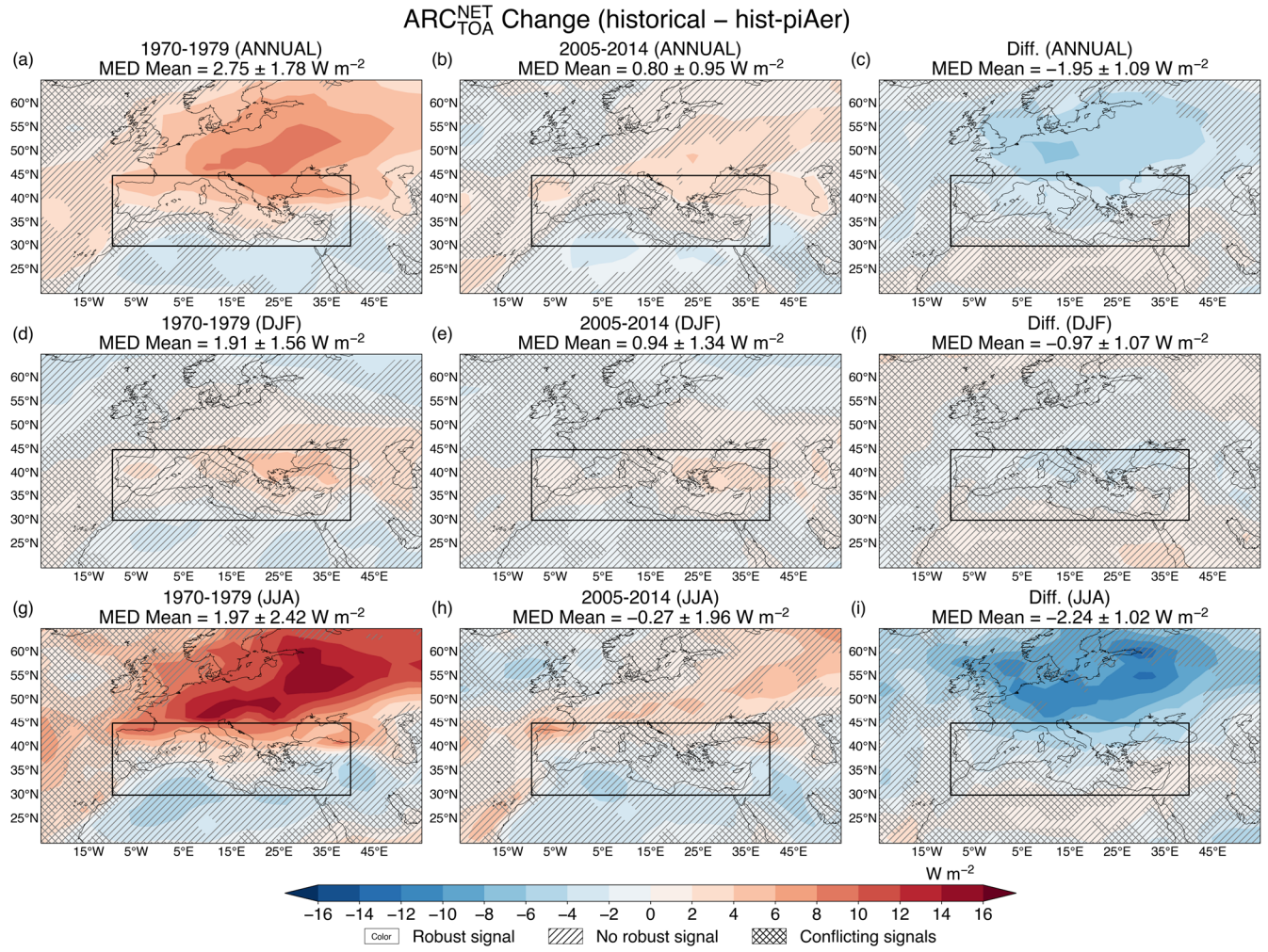

Figure S5. Net ARC_{TOA} due to anthropogenic aerosols over the Mediterranean (calculated from the difference "historical" minus "hist-piAer"). Spatial patterns are presented for the periods 1970-1979 (left column), 2005-2014 (middle column) and their difference (2005-2014 minus 1970-1979; right column) on an annual scale (top row) and in boreal winter (DJF; middle row) and summer (JJA; bottom row). The multi-model ensemble means over the Mediterranean region (shown as a box) are shown along with the inter-model variability (one standard deviation) at the top of each panel. Colored areas without markings indicate robust changes, while hatched (/) and cross-hatched (X) areas indicate non-robust changes and conflicting signals, respectively.

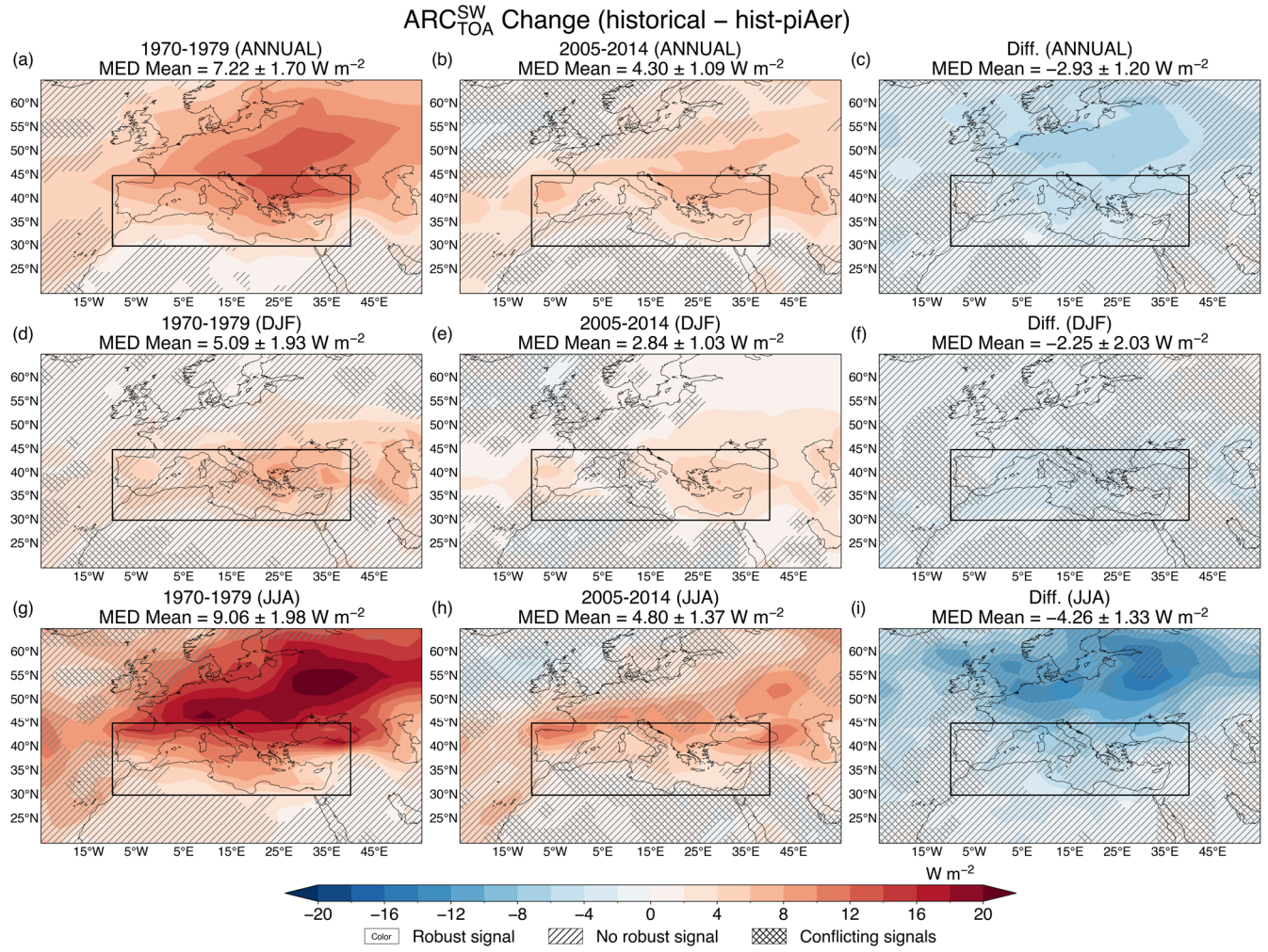

Figure S6. Shortwave (SW) ARC_{TOA} due to anthropogenic aerosols over the Mediterranean (calculated from the difference "historical" minus "hist-piAer"). Spatial patterns are presented for the periods 1970-1979 (left column), 2005-2014 (middle column) and their difference (2005-2014 minus 1970-1979; right column) on an annual scale (top row) and in boreal winter (DJF; middle row) and summer (JJA; bottom row). The multi-model ensemble means over the Mediterranean region (shown as a box) are shown along with the inter-model variability (one standard deviation) at the top of each panel. Colored areas without markings indicate robust changes, while hatched (/) and cross-hatched (X) areas indicate non-robust changes and conflicting signals, respectively.

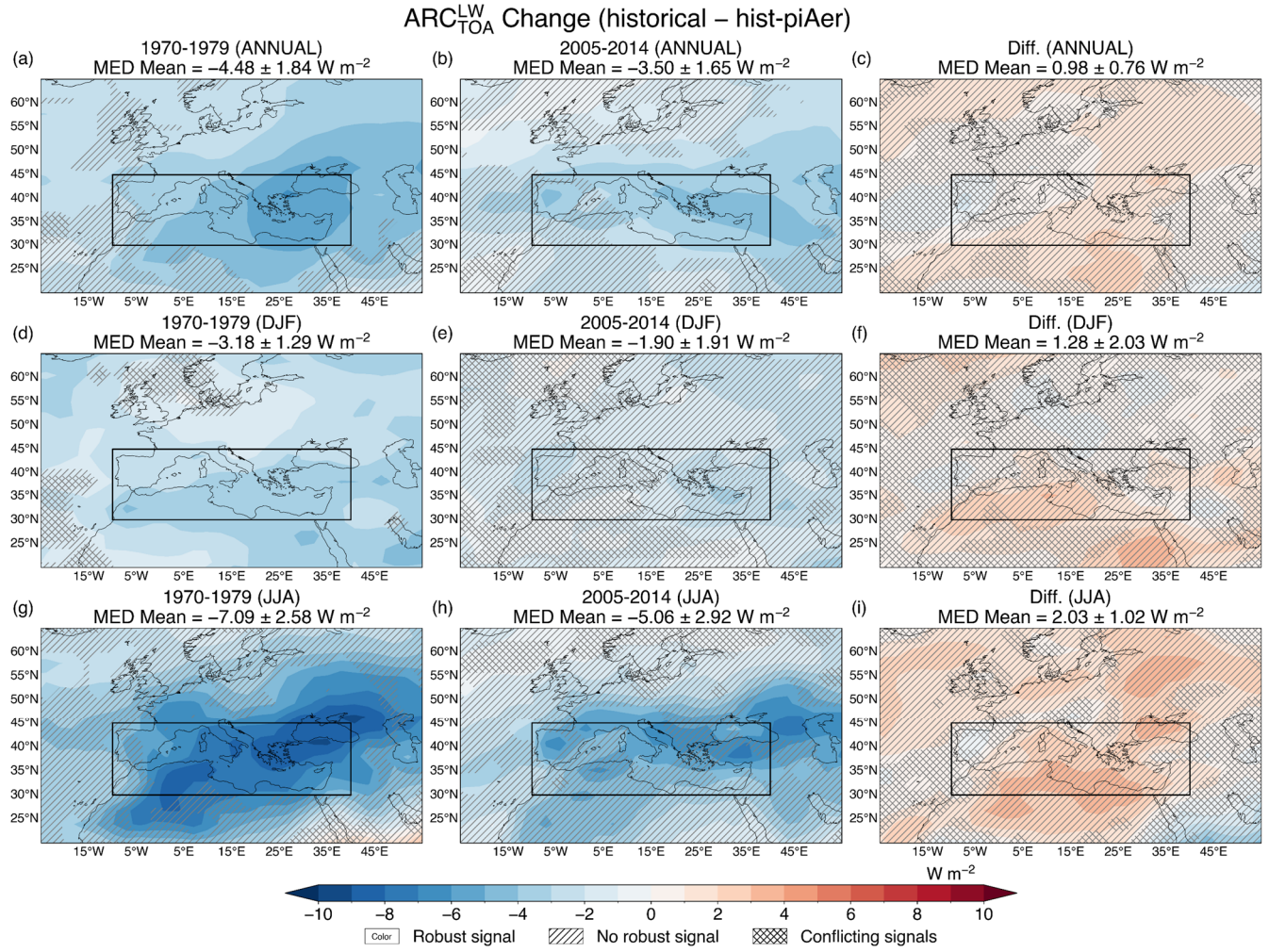

Figure S7. Longwave (LW) ARC_{TOA} due to anthropogenic aerosols over the Mediterranean (calculated from the difference "historical" minus "hist-piAer"). Spatial patterns are presented for the periods 1970-1979 (left column), 2005-2014 (middle column) and their difference (2005-2014 minus 1970-1979; right column) on an annual scale (top row) and in boreal winter (DJF; middle row) and summer (JJA; bottom row). The multi-model ensemble means over the Mediterranean region (shown as a box) are shown along with the inter-model variability (one standard deviation) at the top of each panel. Colored areas without markings indicate robust changes, while hatched (/) and cross-hatched (X) areas indicate non-robust changes and conflicting signals, respectively.

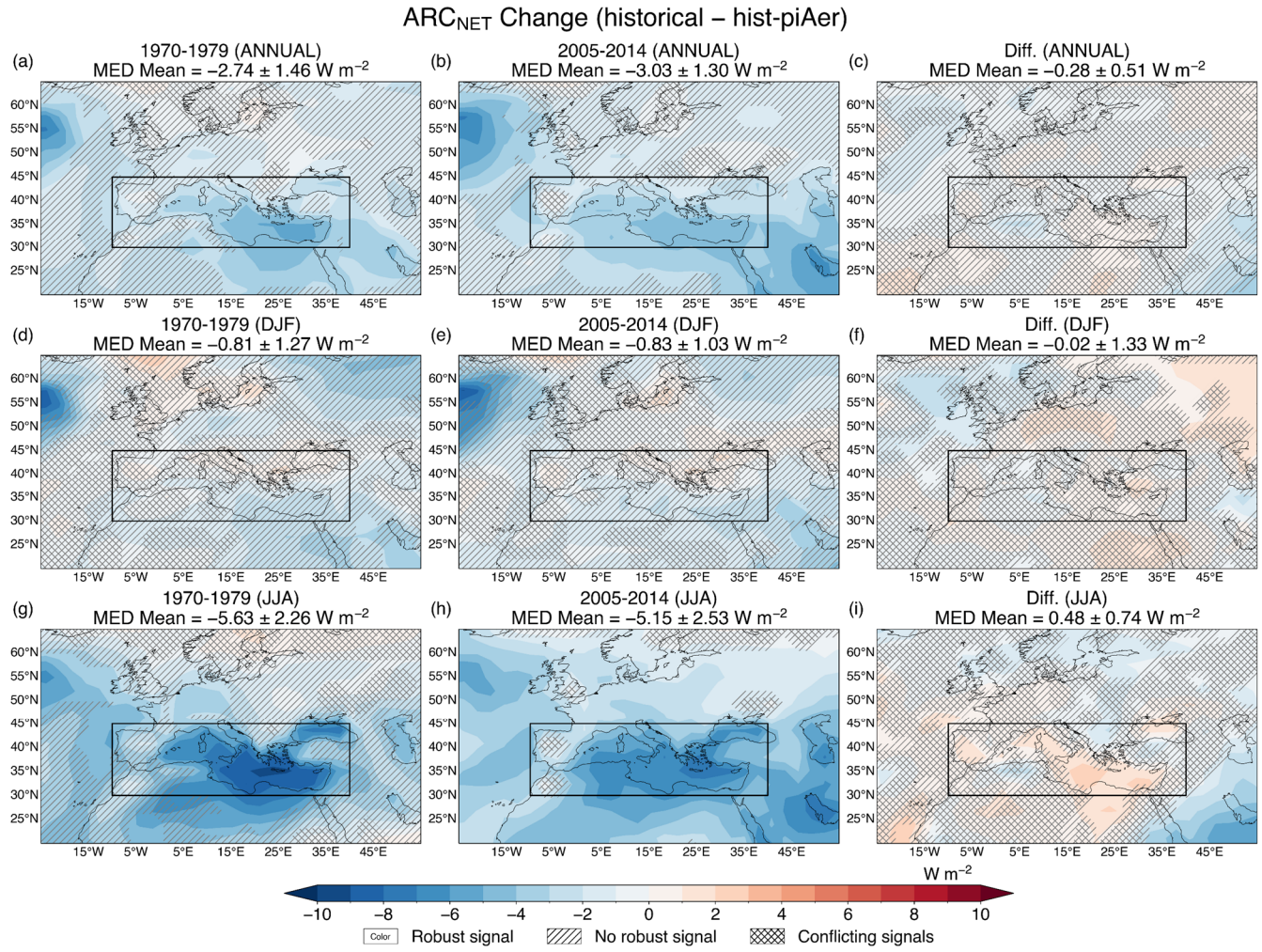

Figure S8. Net ARC for the entire atmospheric column due to anthropogenic aerosols over the Mediterranean (calculated from the difference "historical" minus "hist-piAer"). Spatial patterns are presented for the periods 1970-1979 (left column), 2005-2014 (middle column) and their difference (2005-2014 minus 1970-1979; right column) on an annual scale (top row) and in boreal winter (DJF; middle row) and summer (JJA; bottom row). The multi-model ensemble means over the Mediterranean region (shown as a box) are shown along with the inter-model variability (one standard deviation) at the top of each panel. Colored areas without markings indicate robust changes, while hatched (/) and cross-hatched (X) areas indicate non-robust changes and conflicting signals, respectively.

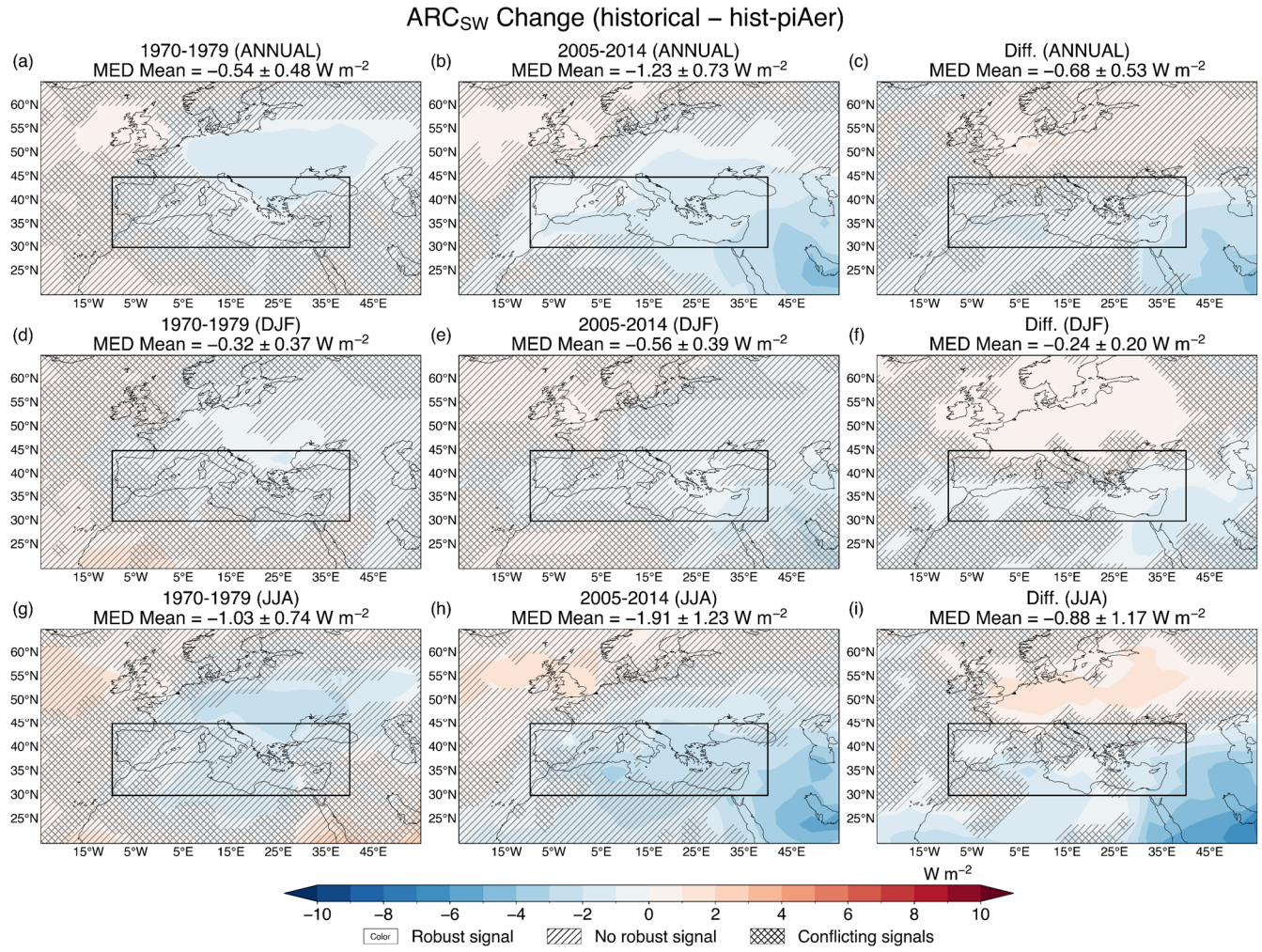

Figure S9. Shortwave (SW) ARC for the entire atmospheric column due to anthropogenic aerosols over the Mediterranean (calculated from the difference "historical" minus "hist-piAer"). Spatial patterns are presented for the periods 1970-1979 (left column), 2005-2014 (middle column) and their difference (2005-2014 minus 1970-1979; right column) on an annual scale (top row) and in boreal winter (DJF; middle row) and summer (JJA; bottom row). The multi-model ensemble means over the Mediterranean region (shown as a box) are shown along with the inter-model variability (one standard deviation) at the top of each panel. Colored areas without markings indicate robust changes, while hatched (/) and cross-hatched (X) areas indicate non-robust changes and conflicting signals, respectively.

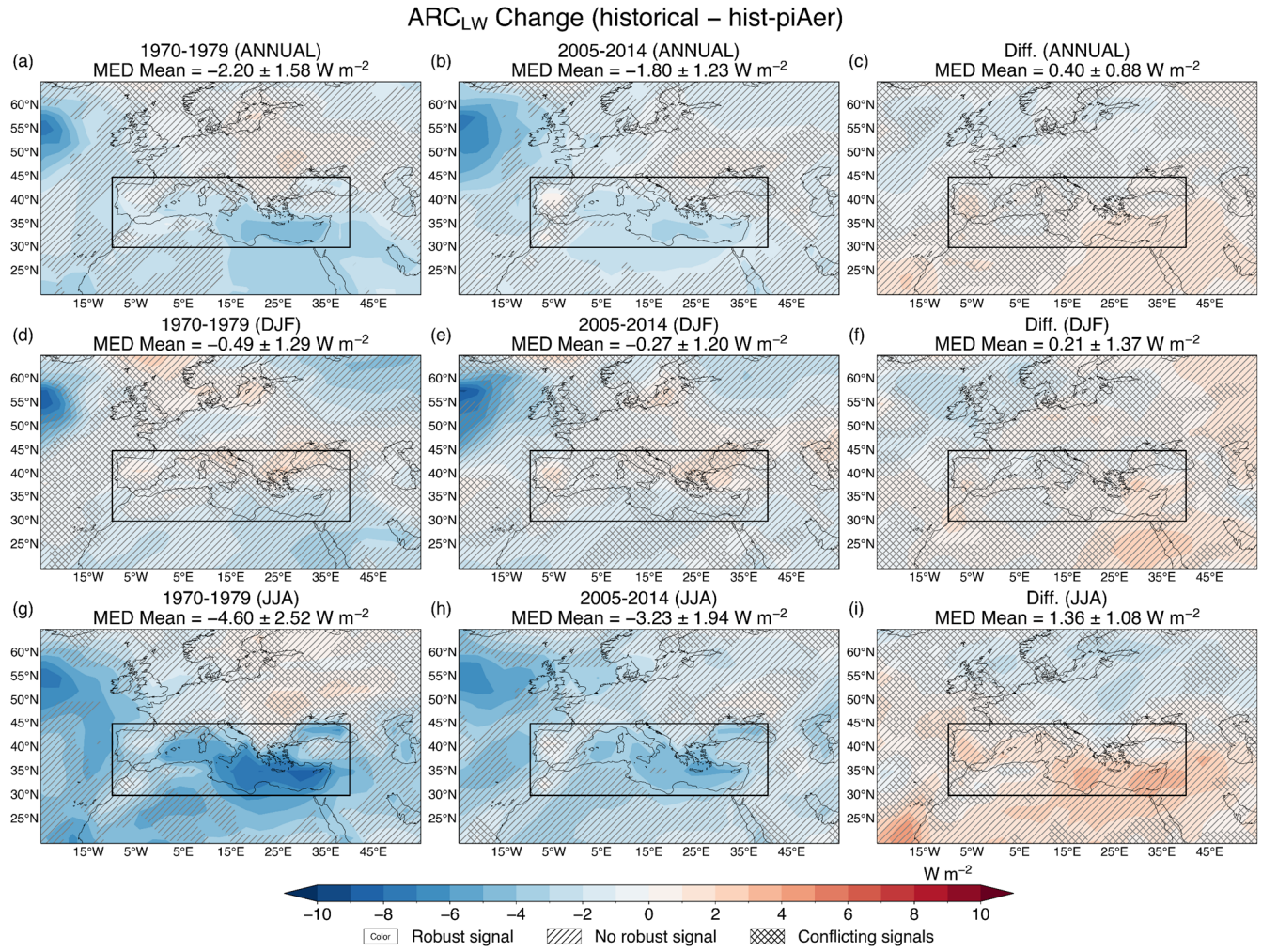

Figure S10. Longwave (LW) ARC for the entire atmospheric column due to anthropogenic aerosols over the Mediterranean (calculated from the difference "historical" minus "hist-piAer"). Spatial patterns are presented for the periods 1970-1979 (left column), 2005-2014 (middle column) and their difference (2005-2014 minus 1970-1979; right column) on an annual scale (top row) and in boreal winter (DJF; middle row) and summer (JJA; bottom row). The multi-model ensemble means over the Mediterranean region (shown as a box) are shown along with the inter-model variability (one standard deviation) at the top of each panel. Colored areas without markings indicate robust changes, while hatched (/) and cross-hatched (X) areas indicate non-robust changes and conflicting signals, respectively.

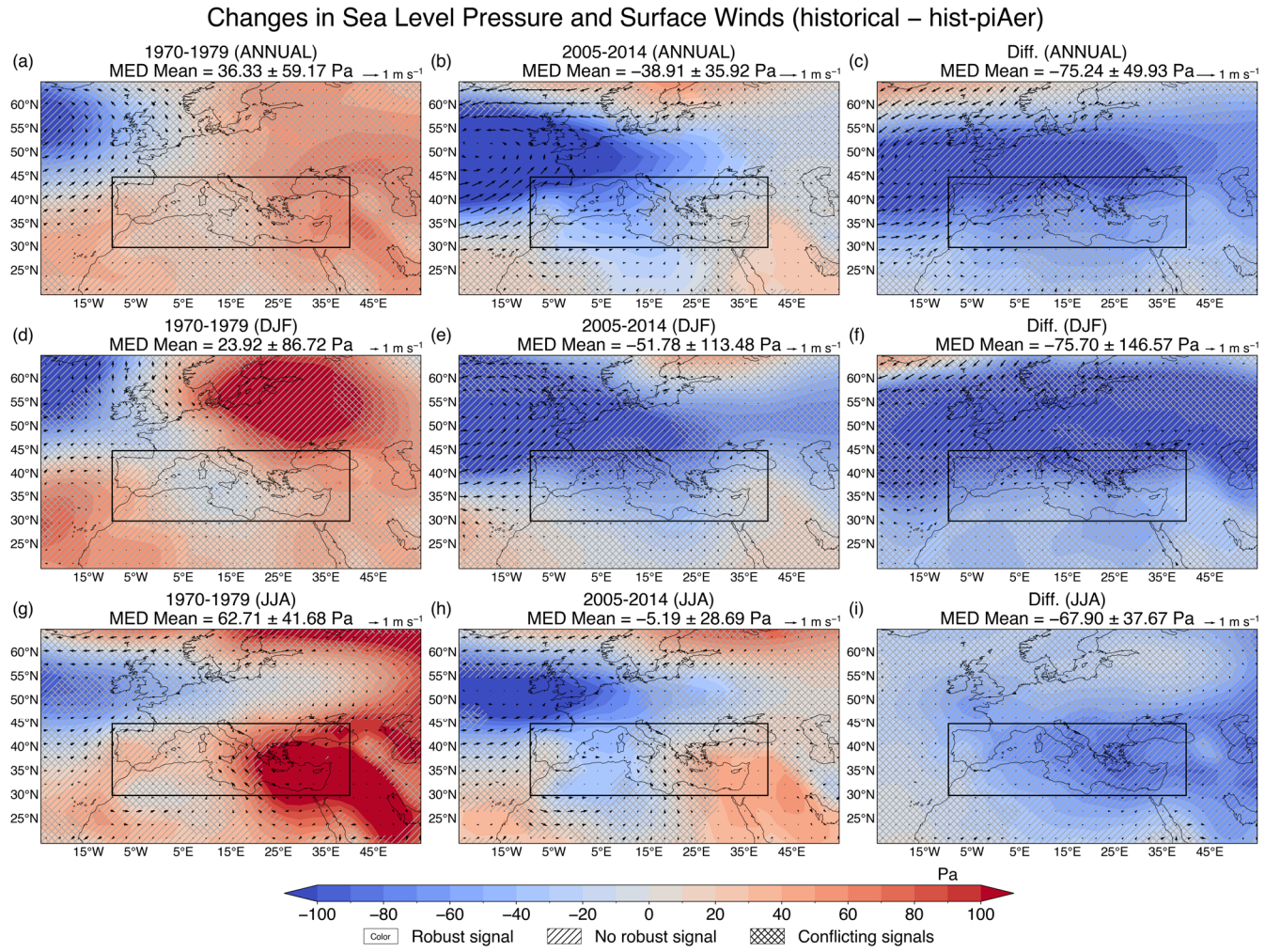

Figure S11. Changes in sea-level pressure and near-surface winds due to anthropogenic aerosols over the Mediterranean (calculated from the difference "historical" minus "hist-piAer"). Spatial patterns are presented for the periods 1970-1979 (left column), 2005-2014 (middle column) and their difference (2005-2014 minus 1970-1979; right column) on an annual scale (top row) and in boreal winter (DJF; middle row) and summer (JJA; bottom row). The multi-model ensemble means over the Mediterranean region (shown as a box) are shown along with the inter-model variability (one standard deviation) at the top of each panel. Colored areas without markings indicate robust changes, while hatched (/) and cross-hatched (X) areas indicate non-robust changes and conflicting signals, respectively.